

Thermal Transport in One Dimensional Electronic Fluid

R. Samanta,¹ I. V. Protopopov,^{2,3} A. D. Mirlin,^{4,5,6,3} and D.B. Gutman¹

¹*Department of Physics, Bar Ilan University, Ramat Gan 52900, Israel*

²*Department of Theoretical Physics, University of Geneva, 1211 Geneva, Switzerland*

³*Landau Institute for Theoretical Physics, 119334 Moscow, Russia*

⁴*Institut für Nanotechnologie, Karlsruhe Institute of Technology, 76021 Karlsruhe, Germany*

⁵*Institut für Theorie der Kondensierten Materie,*

Karlsruhe Institute of Technology, 76128 Karlsruhe, Germany

⁶*Petersburg Nuclear Physics Institute, 188350 St. Petersburg, Russia*

We study thermal conductivity for one-dimensional electronic fluid. The many-body Hilbert space is partitioned into bosonic and fermionic sectors that carry the thermal current in parallel. For times shorter than bosonic Umklapp time, the momentum of Bose and Fermi components are separately conserved, giving rise to the ballistic heat propagation and imaginary heat conductivity proportional to $T/i\omega$. The real part of thermal conductivity is controlled by decay processes of fermionic and bosonic excitations, leading to several regimes in frequency dependence. At lowest frequencies or longest length scales, the thermal transport is dominated by Lévy flights of low-momentum bosons that lead to a fractional scaling, $\omega^{-\frac{1}{3}}$ and $L^{1/3}$, of heat conductivity with the frequency ω and system size L respectively.

In interacting systems, Wiedemann-Franz law is violated and there is no universal relation between the thermal and electric conductivities. As a result, thermal transport reveals information that can not be accessed by measuring charge transport. Due to experimental and theoretical challenges, thermal transport is far less explored compared to charge transport.

In recent years, the situation started to change, and energy transport was measured in several experiments. The universal value of thermal conductance $g_0 = \pi^2 T/3h$ was observed¹⁻⁴ in various devices with ideal point contacts. Heat Coulomb blockade was observed in⁵, directly demonstrating a controllable energy-charge separation. The propagation of heat in the quantum-Hall-effect regime was intensively investigated⁶⁻¹¹. Frequency dependence of the thermal conductivity was studied in various materials¹²⁻¹⁴.

The thermal transport in low-dimensional classical fluids and 1D anharmonic chains (of which the Fermi-Pasta-Ulam-Tsingou model¹⁵ is a prominent example) has been studied in the framework of (non-linear) fluctuating hydrodynamics. The corresponding renormalization group (RG)¹⁶ or self-consistent mode-coupling¹⁷ analysis predicts that the thermal DC conductivity scales with the system size as $\sigma \sim L^{1/3}$ in 1D models with momentum conservation. This prediction was verified by means of numerical simulations in Ref.¹⁸. The $\sigma \sim L^{1/3}$ behavior of the heat conductivity is closely related to the anomalous broadening, $\Delta x \sim t^{1/z} \sim t^{2/3}$, (on top of ballistic propagation) of the sound peak in the density-density correlation function of the system. The dynamical exponent $z = 3/2$ entering here is a manifestation of the Kardar-Parisi-Zhang (KPZ) fixed point in the RG flow that governs the propagation of the sound mode¹⁹. The KPZ scaling of the density-density correlation function was also predicted (within the classical Gross-Pitaevskii formalism) to occur in 1D Bose gas at finite temperature²⁰. In the context of 1D Fermi systems

the KPZ scaling was advocated in Ref.²¹.

The experimental progress combined with open fundamental questions prompts us to study thermal transport in a 1D quantum electronic fluid. In the low-energy limit such fluids are often described within the Tomonaga-Luttinger model that linearizes the spectrum of fermions near Fermi points and treats the interaction of fermions as point-like. Via the bosonization procedure²², Tomonaga-Luttinger model maps to free bosons with a linear dispersion relation. The Luttinger liquid (LL) fixed point is thus a free theory with essentially trivial kinetics. It turns out however, that the corrections to it, a finite curvature of fermionic spectrum and a finite range of interactions, albeit irrelevant in RG sense, can have profound effect on the low-energy behaviour of the system's *dynamical* correlation functions²³⁻²⁸. Therefore, those perturbations are to be taken into account in the discussion of the thermal conductivity, i.e., the conventional LL paradigm is not sufficient for this problem.

With the aforementioned corrections included, the Tomonaga-Luttinger model turns into an interacting theory both in fermionic and bosonic²⁹⁻³³ languages. One then has to resort to perturbative treatment of the model. Two choices of basis for such a perturbation theory are available³⁴: i) one can choose to work with the bosonized version of the theory treating the nonlinearity of fermionic spectrum (that translates into interaction of bosons) perturbatively; ii) the bosonic theory can be refermionized^{26,34,35} giving rise to the description of the system in terms of fermionic quasiparticles that are related to original electrons via non-linear unitary transformation. In the later approach the curvature of the bosonic spectrum translates into the interaction of fermions³⁶.

It was shown in Ref.³⁴ that the applicability of perturbation theory for *thermal* (with energy of order T) excitations in the fermionic and bosonic approaches de-

depends on temperature. Specifically, the effective mass of fermionic excitations m_* and a length l quantifying the curvature of bosonic spectrum [see Eq. (2)] define a temperature scale $T_{\text{FB}} = 1/m_* l^2$. At $T < T_{\text{FB}}$ the thermal fermions are long-living excitations; the perturbation theory in their interaction is well-behaved and controlled by the small parameter T/T_{FB} . At higher temperatures, $T > T_{\text{FB}}$, the proper thermal excitations are bosons and the bosonic perturbation theory possess a small parameter T_{FB}/T .

In this work we employ the combination of the fermionic and bosonic frameworks to study low-temperature thermal conductivity of the electronic fluid. It turns out that *subthermal* excitations dominate the thermal transport at low frequencies and one is faced with the problem of understanding their kinetics. We show that at lowest frequencies the behavior of thermal conductivity is anomalous and has the universal scaling $\sigma(\omega) \propto \omega^{-\frac{1}{3}}$. This corresponds to length dependent DC thermal conductivity $\sigma(L) \propto L^{\frac{1}{3}}$ consistent with the classical hydrodynamic limit^{16,17}. At higher frequencies, we identify a variety of new regimes characterized by power-law dependence of thermal conductance on frequency, temperature and system size.

We consider a model of spinless right- and left-moving fermions

$$H = \sum_{\eta} \int dx \psi_{\eta}^{\dagger}(x) \left(-i\eta v_F \partial_x - \frac{1}{2m} \partial_x^2 \right) \psi_{\eta}(x) + \frac{1}{2} \int dx dx' g(x-x') \rho(x) \rho(x'), \quad (1)$$

where $g(x)$ is short-range interaction potential, and the total density $\rho(x)$ is a sum of the chiral components, $\rho(x) = \rho_R(x) + \rho_L(x)$. In the low momentum limit ($ql \ll 1$), the interaction potential is $g_q - g_0 \propto q^2 l^2$.

After bosonization, the original Hamiltonian(1) is mapped to an interacting bosonic model^{22,34,37-40}, see Appendix A 1. The interaction between electrons Eq.(1) controls the dispersion of the bosonic modes. At small momenta

$$\omega_q^B = u_q^B |q|, \quad u_q^B = u (1 - l^2 q^2), \quad (2)$$

where $u = v_F \sqrt{1 + g_0/\pi v_F}$ denotes the sound velocity.

We now construct the kinetic equation for bosonic and fermionic quasiparticles. These equations can be derived from the fermionic (1) and bosonized versions of the Hamiltonian in a standard way, see Appendix A 2 and Appendix B 2,

$$\frac{\partial N_{\alpha}(q)}{\partial t} + u_q^{\alpha} \frac{\partial N_{\alpha}(q)}{\partial x} = I_{\alpha,q}[N_{\alpha}]. \quad (3)$$

Here $\alpha = F/B$ specifies the type of the quasi-particles (Fermi/Bose), N_{α} is a distribution function and I_{α} is the collision integral. A combination of two equations (3) permits to extend the Bose-Fermi duality framework³⁴ away from thermal equilibrium. We next linearize the

kinetic equation using the ansatz $N_{\alpha} = n_{\alpha} + \delta N_{\alpha}$, where n_{α} is the quasi-equilibrium distribution and δN_{α} is a deviation from a local equilibrium, see Appendix A 2 (for bosons) and Appendix B 2 (for fermions). To determine the heat conductivity the linearized kinetic equation should be solved for δN_{α} with the temperature gradient introduced into n_{α} . In either fermionic or bosonic approach the energy current can then be computed as

$$J_{\alpha}(\omega) = \int (dq) u_q^{\alpha} \omega_q^{\alpha} \delta N_{\alpha}(q) \quad (4)$$

where for fermions

$$\omega_q^F = \pm uq + q^2/2m^*, \quad u_q^F = \pm u + q/m^*. \quad (5)$$

In Eq. (5) the \pm sign refers to the right and left movers; $(dq) \equiv \frac{dq}{2\pi\hbar}$ and we set $\hbar = 1$ through the manuscript. The explicit formula for the effective mass m_* is given in Appendix A 1.

Before discussing the relaxation of fermionic and bosonic modes in more detail, we note that the model (1) as stated preserves, apart from the charge conservation, also the *difference* of the number of right- and left-moving fermions. In the bosonic language this corresponds to the conservation of the total momentum of the bosonic excitations⁴¹⁻⁴⁴. Correspondingly, the linearized collision integral (both in the fermionic and bosonic formalisms) has a zero mode that gives rise to a ballistic transport of heat⁴⁵. In a more accurate description of the electronic fluid the chiral branches merge at the bottom of the energy band enabling the equilibration of the number of left and right fermions. Within the bosonic description this process corresponds to the Umklapp scattering. The associated time scale is exponentially long⁴¹⁻⁴⁴

$$\tau_U^{-1} \sim T^{3/2} \epsilon_F^{-1/2} e^{-\frac{\epsilon_F}{T}}. \quad (6)$$

Here $\epsilon_F \sim mv_F^2$ is an ultraviolet energy scale and we omitted a non-universal numerical coefficient that is determined by interaction strength and by details of the spectrum at the bottom of the band. The contribution of the (almost) zero mode associated to the conservation of the bosonic momentum can then be extracted either in fermionic or bosonic framework^{46,47}

$$\sigma^{\text{bal}}(\omega) = \frac{\pi}{3} \frac{uT}{i\omega + \tau_U^{-1}}. \quad (7)$$

At $\omega\tau_U \gg 1$, $\sigma^{\text{bal}}(\omega)$ is purely imaginary and does not contribute to the dissipative real part of the total thermal conductance. In the opposite limit, $\omega\tau_U \ll 1$ the contribution of $\sigma^{\text{bal}}(\omega)$ becomes a (large) frequency-independent constant, $\sigma^{\text{bal}} = \pi\tau_U uT/3$.

Let us now turn to the analysis of the relaxing modes in the kinetic equation (3). Employing the relaxation-time approximation for its solution we find

$$\text{Re } \sigma^B(\omega) \simeq \frac{T^4 l^4}{u^2} \text{Re} \int_0^{T/u} \frac{(dq)}{\tau_B^{-1}(q) - i\omega}, \quad (8)$$

for the bosonic and

$$\text{Re } \sigma^F(\omega) \simeq \frac{T^2}{m_*^2 u^2} \text{Re} \int_0^{T/u} \frac{(dq)}{\tau_F^{-1}(q) - i\omega}, \quad (9)$$

for the fermionic representation of the theory, respectively, see Appendix A 3 and Appendix B 3. In Eqs. (8) and (9), $\tau_B(q)$ and $\tau_F(q)$ denote the relaxation times for the bosons and fermions. Note, that the prefactors in Eqs. (8) and (9) match at $T = T_{\text{FB}}$, which is a manifestation of Bose-Fermi duality³⁴. One thus might think that for $T > T_{\text{FB}}$ only bosonic excitations are relevant, and for $T < T_{\text{FB}}$ only fermionic ones. However, this is not true. As we discuss below, the bosonic lifetime $\tau_B(q)$ diverges in low q limit, while $\tau_F(q)$ remains constant. This makes the two channels of heat transport profoundly different: the bosonic one *always* dominates the low-frequency thermal conductivity, irrespectively of the relation between T and T_{FB} .

Equations (8) and (9) represent contributions of bosonic and fermionic quasiparticles to the thermal conductivity. Thus, taking into account also the ballistic contribution σ^{bal} discussed above, we approximate the total thermal conductivity of the electronic fluid by

$$\sigma(\omega) = \sigma^{\text{bal}}(\omega) + \sigma'(\omega), \quad (10)$$

$$\sigma'(\omega) = \sigma^F(\omega) + \sigma^B(\omega) \simeq \max[\sigma^F(\omega), \sigma^B(\omega)]. \quad (11)$$

To evaluate Eqs. (8) and (9), one needs to compute the decay rates $\tau_\alpha^{-1}(q)$ for the fermionic and bosonic sectors and $q \lesssim T/u$. Let us discuss the bosonic excitations first. The simplest process of the bosonic decay obeying energy and momentum conservation is shown in the left panel of Fig.1. It corresponds to the decay of one boson mode into three and involves three bosons of the same chirality (e.g. right) and one boson of the opposite chirality^{34,50}. The resulting decay rate of subthermal bosons is given by (see Appendix A 2) we omit numerical factors)

$$\frac{1}{\tau_B(q)} \sim \begin{cases} \frac{\gamma q^{\frac{5}{3}} T^2}{u^5 l^{\frac{4}{3}} m_*^4}, & q < \frac{l^2 T^3}{u^3}, \\ \frac{\gamma q^2 T^3}{m_*^4 u^6}, & \frac{l^2 T^3}{u^3} < q < \frac{T}{u}. \end{cases} \quad (12)$$

Here $\gamma = \alpha^2(1 + \alpha)^2$ is a dimensionless interaction parameter related to the LL parameter K_0 by the relation $\alpha = \frac{1 - K_0^2}{3 + K_0^2}$. The second line of Eq. (12) agrees with Ref.⁵⁰; the $q^{5/3}$ scaling as in the first line was obtained in the context of classical anharmonic chains^{48,49}. Note that the process shown in the left panel of Fig. 1 can be interpreted as either a contribution to the relaxation of one of the ‘‘majority’’ bosons (q) or of the ‘‘minority’’ boson (p). Kinematic constraints imply $p \ll q$. As a result, the second contribution is exponentially suppressed at large momenta of the relaxing boson. It however dominates at small momenta and gives rise to the first line in Eq. (12).

The process on the left panel of Fig. 1 can be viewed as a decay of a right boson q into two other right bosons assisted by a left mover p . The participation of the later is required by kinematic constraints on the Fermi

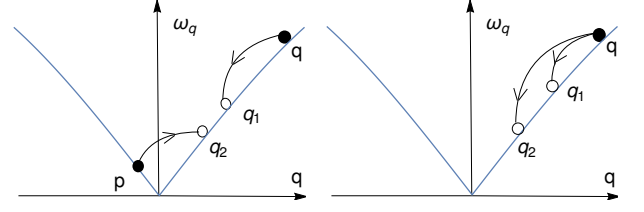


FIG. 1: Left: Two-into-two bosonic scattering process involving three bosons of the same chirality and one boson of opposite chirality. Right: The self-consistent decay process of one boson into two, yielding the decay rate $\tau^{-1}(q) \propto q^{3/2}$ for $q < q_{\text{thr}}$.

golden-rule level. However, once the bosonic spectrum is broadened by some relaxation processes, direct decay of a bosonic excitation into two bosons of the same chirality becomes possible. In particular, at $q < q_{\text{thr}}$, where q_{thr} is a threshold momentum,

$$q_{\text{thr}} = \frac{T^{1/3}}{u m_*^{2/3} l^{4/3}} \equiv \frac{T}{u} \left(\frac{T_{\text{FB}}}{T} \right)^{2/3}, \quad (13)$$

the *self-consistent* treatment of the process shown in the right panel of Fig. 1 provides the dominant contribution to the relaxation of bosons^{21,51,52} (see Appendix A 2),

$$\tau_B^{-1}(q) \sim q^{3/2} m_*^{-1} \sqrt{T/u}, \quad q < q_{\text{thr}}. \quad (14)$$

Summarising the above analysis, we get

$$\frac{1}{\tau_B(q)} \sim \begin{cases} q^{3/2} \frac{\sqrt{T/u}}{m_*}, & q < q_{\text{thr}}, \\ \frac{\gamma q^{\frac{5}{3}} T^2}{u^5 l^{\frac{4}{3}} m_*^4}, & q_{\text{thr}} < q < \frac{l^2 T^3}{u^3}, \\ \frac{\gamma q^2 T^3}{m_*^4 u^6}, & \max\left\{\frac{l^2 T^3}{u^3}, q_{\text{thr}}\right\} < q < \frac{T}{u}. \end{cases} \quad (15)$$

The last two regimes in Eq. (15) can be absent if the corresponding momentum interval vanishes. Specifically, for $T < T_{\text{FB}}$ the bosonic relaxation rate is always given by the first line in Eq. (15). The intermediate regime, $q_{\text{thr}} < q < \frac{l^2 T^3}{u^3}$, disappears at $T < T_H = u^{\frac{3}{4}} l^{-\frac{5}{4}} m_*^{-\frac{1}{4}}$.

As for the fermionic excitations, their lifetime was discussed in Refs.^{26,27,34,53}. It is given by

$$\frac{1}{\tau_F(q)} \sim \frac{\gamma l^4 T^7}{m_*^2 u^8}, \quad q < \frac{T}{u}. \quad (16)$$

Note that while the bosonic decay rate vanishes at $q \rightarrow 0$ limit, the fermionic rate remains finite. This implies that the low-frequency behavior of the thermal conductivity is dominated by bosons.

We now calculate the real part of thermal conductivity as a function of ω and T , using decay rates Eqs.(15) and (16). For $T < T_{\text{FB}}$, we find

$$\sigma'(\omega) \sim \begin{cases} \frac{T^{\frac{1}{3}} l^4 u^{-\frac{5}{3}} m_*^{\frac{2}{3}}}{\omega^{\frac{1}{3}}}, & \omega < \frac{\gamma^3 T^{23} m_*^2 l^{24}}{u^{20}}, \\ \frac{u^5}{\gamma T^4 l^4}, & \frac{\gamma^3 T^{23} m_*^2 l^{24}}{u^{20}} < \omega < \frac{\gamma l^4 T^7}{m_*^2 u^8}, \\ \frac{1}{\omega^2} \frac{\gamma T^{10} l^4}{u^{11} m_*^4}, & \frac{\gamma l^4 T^7}{m_*^2 u^8} < \omega. \end{cases} \quad (17)$$

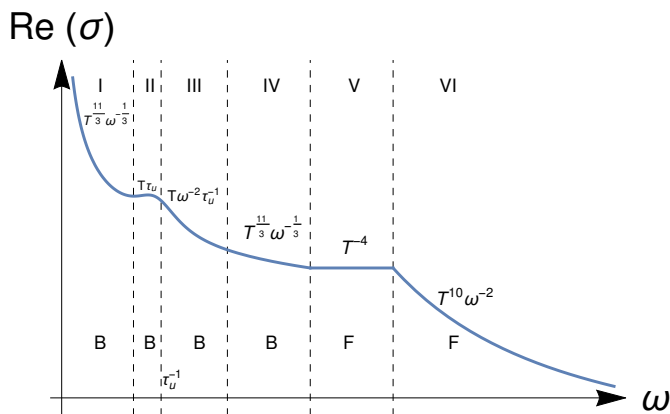


FIG. 2: $\text{Re } \sigma(\omega)$ at $T < T_{\text{FB}}$. For each regime, the T and ω scaling is shown. Label F and B indicates whether the dominant contribution comes from the fermionic or bosonic sector. In region II and III the contribution of the momentum zero mode (7) is dominant, while other regions are dominated by finite energy modes, Eq.(17). For lowest ω , region I, the $\omega^{-1/3}$ dependence translates into the $L^{1/3}$ scaling of $\sigma(L)$, analogous to that obtained for classical fluids^{16,17}.

For details of the calculations and results for $T > T_{\text{FB}}$ see Appendix C1. To obtain the overall picture, the “ballistic” contribution (7) should be taken into account. At sufficiently high frequencies, $\omega \gg 1/\tau_U$, the ballistic mode associated with the conservation of the momentum of bosonic excitations does not contribute to the real part of $\sigma(\omega)$ and $\sigma(\omega) \approx \sigma'(\omega)$. At $\tau_U \omega \lesssim 1$ the ballistic channel of the energy propagation becomes gapped and contributes an exponentially large but frequency-independent constant $\sigma^{\text{bal}} \simeq \pi u T \tau_U / 3$ to the thermal conductance.

The resulting behavior of $\sigma(\omega)$ is shown in Fig.2 for $T < T_{\text{FB}}$ and in Figs. 1 and 2 of Appendix C1 for $T > T_{\text{FB}}$. At $\omega < 1/\tau_U$, we observe a universal $\omega^{-1/3}$ scaling of $\sigma(\omega)$. This behavior can be traced back to the contribution of bosons with momentum $q \ll T/u$ that have the relaxation rate specified in first line of Eq. (15). It is consistent with the predictions of the fluctuating hydrodynamics. This is to be expected as strongly sub-thermal bosonic modes correspond to classical density waves of the hydrodynamic theory.

We now discuss the scaling of the DC conductivity with the system size L . In contrast to the frequency scaling, the contribution of the zero mode associated to the conservation of the bosonic momentum is always real. In fact at scales shorter than L_U the entire DC thermal conductance is dominated by this *ballistic* contribution, $\sigma(L) = \pi T L / 6$, with the other modes providing only sub-leading corrections. The situation changes in the limit $L \gg L_U$ where the contribution of the zero mode becomes a size-independent constant, and non-zero modes start to be dominant.

As was found above, the thermal conductivity $\sigma(\omega \rightarrow$

0) is governed by bosons. In this limit, the bosonic life-time diverges as power law $\tau^{-1}(q) \propto q^z$. In our case $z = 3/2$, that is consistent with KPZ scaling²¹. The divergence of the life time implies that bosons with momentum below $q < L^{-1/z}$ propagate through the system almost ballistically. The contribution of these bosons to the thermal conductance can be estimated as

$$G(L) \sim L^{-1/z}. \quad (18)$$

This implies that for $z = 3/2$ the conductivity scales as $\sigma(L) = L^{1/3}$. Note that this is a manifestation of the Lévy-flight character of the energy transport in the system, cf. Ref.¹⁷. To find the corresponding Lévy-flight distribution function, one needs to relate z to the Lévy-flight parameter α . This can be done by comparing the diffusion coefficient D_E of the Lévy-flight process with the thermal conductivity computed above. The thermal conductance G is related to the energy diffusion coefficient as $G = \sigma/L \sim D_E/L$. To estimate D_E we compute

$$D_E = \frac{\langle x^2 \rangle}{t} \sim \int_0^{L/u} dx x^2 x^{-\alpha-1} \sim L^{2-\alpha}, \quad (19)$$

where we used that the tails of the Lévy distribution function at time t decay with distance as $x^{-\alpha-1}t$. Comparing Eqs. (18) and (19), we obtain the following relation between the exponent z controlling decay rate and α of Lévy flight, $1 - \alpha = -z^{-1}$, so that the conductivity scales as $\sigma \sim L^{2-\alpha} = L^{1-z^{-1}}$. For $z = \frac{3}{2}$, the Lévy parameter $\alpha = 5/3$ and $\sigma(L)$ scales as $L^{\frac{1}{3}}$. Note that the scaling in L for Lévy-flight regime can be obtained from the scaling in ω by the replacement $\omega \rightarrow u/L$. The $L^{1/3}$ scaling agrees with the one found in classical fluids^{16,17}.

To summarize, we computed the thermal conductivity of 1D electronic fluid as a function of frequency ω , temperature T , and system length L . For energy scales below bosonic Umklapp time, the momentum of bosonic and fermionic fluids are separately conserved. The momentum zero mode give rise to the ballistic heat conductivity Eq.(7). This corresponds to purely imaginary $\sigma(\omega)$ and results in the LL thermal conductance $\pi^2 T / 3 h^4$ for a finite sample. The massive modes of the fermionic and bosonic collision integrals contribute to the real part of the heat conductivity, yielding subleading in $1/L$ corrections to the thermal conductance. However, they may be detected via measuring real part of $\sigma(\omega)$ at $\omega > u/L$. The real part of $\sigma(\omega)$ exhibits several regimes. For temperatures $T < T_{\text{FB}}$ it is determined by fermionic modes for not too low frequencies, see regions V and VI in Fig. 2. At the lowest frequencies, the conductivity is determined by low-momentum bosonic modes, yielding $\sigma(\omega) \propto \omega^{-1/3}$. The length dependence of the thermal conductance depends on the relation between L and the bosonic umklapp length L_U . For $L \ll L_U$, the transport is ballistic, $\sigma(L) \propto L$, as expected for LL. On the other hand, for $L \gg L_U$, we find $\sigma(L) \propto L^{1/3}$, as expected for a classical fluid^{16,17}.

We close by briefly discussing prospective research directions. First, while our computations were done within

kinetic theory, these results can be found also within the hydrodynamic approach. While for $L > L_U$ the hydrodynamic theory has three modes (particle-number, momentum, and energy conservation), for $L < L_U$ the number of modes is four, due to the additional zero mode discussed above. In both regimes, kinetic coefficients are expected to be anomalous. The hydrodynamic framework is particularly convenient for computing scaling functions describing heat conductivity and pulse evolution⁵⁴. Second, whereas our computations were done for a strictly 1D system, we expect that an anomalous scaling of heat conductance should hold also for other low-dimensional

quantum electronic fluids (quasi-1D and 2D geometries).

Note added: Shortly after our paper was submitted, a related preprint⁵⁵ appeared, which addresses the same problem solely within the fermionic approach. Results of Ref.⁵⁵ for $\sigma(\omega)$ match ours in what concerns the ‘‘plateaus’’ II and V in Fig. 2 but do not capture other regions, where $\sigma(\omega)$ is controlled by a slow relaxation of bosonic modes.

Acknowledgements: D. G. was supported by ISF (grant 584/14) and Israeli Ministry of Science, Technology and Space.

Appendix A: Kinetic theory for bosonic excitations

1. Brief details of bosonization

In this section we briefly recap the bosonization approach for electrons with a finite curvature^{22,34,38–40}. The system of interacting electrons in one dimension is described by the microscopic Hamiltonian

$$H = \sum_{\eta=R/L} \int dx \psi_{\eta}^{\dagger}(x) \left(-i\eta v_F \partial_x - \frac{1}{2m} \partial_x^2 \right) \psi_{\eta}(x) + \frac{1}{2} \int dx dx' g(x-x') \rho(x) \rho(x'). \quad (\text{A1})$$

After the bosonisation procedure, the Hamiltonian can be represented in terms of the density field,

$$H = \sum_{\eta} \int dx : \left(\pi v_F \rho_{\eta}^2(x) + \frac{2\pi^2}{3m} \rho_{\eta}^3(x) \right) :_B + \frac{1}{2} \int dx dx' g(x-x') : \rho(x) \rho(x') :_B. \quad (\text{A2})$$

Here $::_B$ stands for normal ordering with respect to the bosonic modes. The coupling between left and right chiral sectors can be eliminated up to a cubic level by performing unitary transformations, $R = U \rho_R U^+$, $L = U \rho_L U^+$, see Ref.³⁴ for the details.

After the rotation, the bosonic Hamiltonian reads

$$H = : \frac{\pi}{L} \sum_q u_q R_q R_{-q} + \frac{1}{L^2} \sum_{\mathbf{q}} \Gamma_{\mathbf{q}}^{B,RRR} R_{q_1} R_{q_2} R_{q_3} + \frac{1}{L^3} \sum_{\mathbf{q}} \Gamma_{\mathbf{q}}^{B,RRRL} R_{q_1} R_{q_2} R_{q_3} L_{q_4} :_B + (R \leftrightarrow L). \quad (\text{A3})$$

The bosonic vertices $\Gamma_{\mathbf{q}}$ in Eq.(A3) in the low momentum limit ($ql \ll 1$) are

$$\Gamma_{\mathbf{q}}^{B,RRR} = \frac{2\pi^2}{3m_*} \left(1 - \frac{\alpha l^2}{2} (q_1^2 + q_2^2 + q_3^2) \right), \quad \Gamma_{\mathbf{q}}^{B,RRRL} = \frac{4\pi^3 \alpha}{3m_*^2 u} \left[1 - \frac{3\alpha}{2} + \frac{15}{4} l^2 \frac{q_1 q_2 q_3}{q_4} \right]. \quad (\text{A4})$$

Here $m_* = \frac{4\sqrt{K_0}}{3+K_0} m$ is renormalised mass of the electron, $\alpha = \frac{1-K_0^2}{3+K_0^2}$ is dimensionless interaction strength, and K_0 is LL parameter. Next, we employ the Hamiltonian (A2) to derive a kinetic equation for the bosonic distribution function.

2. Linearization of kinetic equation for bosons

The Fourier components of the densities $R(x)$ and $L(x)$ can be identified with bosonic creation and annihilation operators via

$$\begin{aligned} R_q &= \sqrt{\frac{L|q|}{2\pi}} (\Theta(q) b_q + \Theta(-q) b_{-q}^{\dagger}), \\ L_q &= \sqrt{\frac{L|q|}{2\pi}} (\Theta(-q) b_q + \Theta(q) b_{-q}^{\dagger}). \end{aligned} \quad (\text{A5})$$

The bosonic distribution $N_B(q, x, t)$ is defined as

$$N_B(q, x, t) = \frac{1}{2\pi} \int_{-\infty}^{\infty} d(q_1 - q_2) e^{i(q_1 - q_2)x} \langle b_{q_1}^+(t) b_{q_2}(t) \rangle, \quad (\text{A6})$$

where $q = (q_1 + q_2)/2$ and the operators b_q and b_q^+ are defined in Eq.(A5). Using a standart Keldysh formalism^{56,57} one derives the kinetic equation for bosons

$$\frac{\partial N_q}{\partial t} + u_q \frac{\partial N_q}{\partial x} = \mathcal{I}_{\text{out}}[N_q] + \mathcal{I}_{\text{in}}[N_q]. \quad (\text{A7})$$

Here $u_q = \frac{d\omega_q}{dq}$ is the sound velocity; the incoming and outgoing parts of the collision integral are

$$\begin{aligned} \mathcal{I}_{\text{out}}[N_q] &= - \sum_{p, q_1, q_2} W_{q, p; q_1, q_2} N_q N_p (1 + N_{q_1})(1 + N_{q_2}), \\ \mathcal{I}_{\text{in}}[N_q] &= \sum_{p, q_1, q_2} W_{q, p; q_1, q_2} (1 + N_q)(1 + N_p) N_{q_1} N_{q_2}. \end{aligned}$$

The matrix element

$$W_{q_1', q_2'; q_1, q_2} = \frac{\gamma}{m_*^4 u^2} |q_1 q_2 q_1' q_2'| \delta_{q_1' + q_2', q_1 + q_2} \delta(\omega_{q_1} + \omega_{q_2} - \omega_{q_1'} - \omega_{q_2'}), \quad (\text{A8})$$

where we defined $\gamma = \alpha^2(1 + \alpha)^2$.

If the deviations from the equilibrium are small, one can linearise the collision integral. It is conveniently done in the following parametrization:

$$N_q = n_q + g_q f_q, \quad g_q = \sqrt{n_q(1 + n_q)}. \quad (\text{A9})$$

Here f_q represents the deviation of the distribution function from the local equilibrium distribution n_q . The linearised kinetic equation reads

$$\frac{\partial f_q}{\partial t} + \frac{u_q}{g_q} \frac{\partial n_q}{\partial T} \nabla T = - \frac{\gamma}{m_*^4 u^2} \sum_{p, q_1, q_2} |qpq_1q_2| \left(\frac{f_q}{g_q} + \frac{f_p}{g_p} - \frac{f_{q_1}}{g_{q_1}} - \frac{f_{q_2}}{g_{q_2}} \right) g_p g_{q_1} g_{q_2} \delta(\omega_q + \omega_p - \omega_{q_1} - \omega_{q_2}) \delta_{q+p, q_1+q_2}. \quad (\text{A10})$$

It is convenient to define a dimensionless momentum $x = \frac{u}{2\pi} \frac{q}{T}$. We now expand Eq.(A10) keeping the lowest order in lT/u . After Fourier transforming with respect to time and implementing the delta functions in Eq.(A10) one finds

$$i\omega f(x) + S(x) = \int_{-\infty}^{\infty} dy \mathcal{K}(x, y) f(y). \quad (\text{A11})$$

Here the source term

$$S(x) = \frac{u}{T} \nabla T \frac{\pi x}{\sinh(\pi|x|)} \left(1 + \frac{4\pi^2 l^2 T^2}{u^2} x^2 [\pi x \coth \pi x - 4] \right). \quad (\text{A12})$$

Note that the source is an odd function, $S(-x) = -S(x)$, and therefore has a finite component along the momentum zero mode and no component along the energy zero mode. For this reason the momentum zero mode is essential for low energy transport. The kernel $\mathcal{K}(x, y)$ is composed of local and non local parts

$$\mathcal{K}(x, y) = \mathcal{K}_1(x) \delta(x - y) + \mathcal{K}_2(x, y). \quad (\text{A13})$$

The local part is

$$\mathcal{K}_1(x) = \begin{cases} \frac{\gamma T^{11/3} x^{5/3} l^{-4/3}}{m_*^4 u^{20/3}}, & x \ll \frac{l^2 T^2}{u^2}, \\ \frac{\gamma T^5}{m_*^4 u^8} \frac{1}{6} x^2 (x^2 + 1), & x > \frac{l^2 T^2}{u^2}. \end{cases} \quad (\text{A14})$$

The non local part of the collision integral

$$\mathcal{K}_2(x, y) = \theta(xy) \frac{\gamma T^5}{m_*^4 u^8} \left(\frac{xy(x+y)}{\sinh[\pi(x+y)]} - \frac{xy(x-y)}{\sinh[\pi(x-y)]} \right) + \theta(-xy) \mathcal{H}(x, y).$$

Here

$$\mathcal{H}(x, y) = \frac{\gamma T}{l^4 m_*^4 u^4} \frac{x^2 g_{q'_1} g_{q'_2}}{|y| \sqrt{y^2 + \frac{2u^2 x}{3l^2 \pi^2 T^2 |y|}}} + \frac{\gamma T}{l^4 m_*^4 u^4} \frac{x^2 g_{q_1} g_{q_2}}{|y| \sqrt{y^2 - \frac{2u^2 x}{3l^2 \pi^2 T^2 |y|}}} \theta \left(|y| - \left(\frac{2u^2 x}{3l^2 \pi^2 T^2} \right)^{\frac{1}{3}} \right) + (x \leftrightarrow y),$$

where the function $g_x \equiv \frac{1}{2 \sinh(\pi|x|)}$ and $q_{1,2} = \frac{1}{2} \left(y \pm \sqrt{y^2 - \frac{2u^2 x}{3l^2 \pi^2 T^2 |y|}} \right)$, $q'_{1,2} = \frac{1}{2} \left(\pm y - \sqrt{y^2 + \frac{2u^2 x}{3l^2 \pi^2 T^2 |y|}} \right)$. Employing Eqs.(A13,A14), on the level of diagonal approximation, we find the bosonic decay rates

$$\frac{1}{\tau_B(q)} = \begin{cases} \frac{\gamma q^{\frac{5}{3}} T^2}{u^5 l^{\frac{4}{3}} m_*^4}, & q < \frac{l^2 T^3}{u^3}, \\ \frac{\gamma q^2 T^3}{m_*^4 u^6}, & \frac{l^2 T^3}{u^3} < q < \frac{T}{u}, \\ \frac{\gamma q^4 T}{m_*^4 u^4}, & q > \frac{T}{u}. \end{cases} \quad (\text{A15})$$

The bosonic decay rates (12) have been computed in Refs.^{34,48,50}. The analytic computation of a decay rate with the full kernel Eq.(A13) is very challenging. However, the numerical analysis we performed showed that results for the decay rate in the small momentum limit found within the full collision integral and those computed within the diagonal approximation agree.

Now we discuss the bosonic vertices $\Gamma_{\mathbf{q}}^{B,RRR}$ and $\Gamma_{\mathbf{q}}^{B,LLL}$, that describe three boson interaction Eq.(A4). The treatment of these vertices on the golden rule level is subtle, and for the bosonic spectrum in the absence of broadening the answer is ill-defined. However, if the broadening of the spectrum is computed self-consistently^{51,52} one finds

$$\frac{1}{\tau_s(q)} = \begin{cases} q^{3/2} \frac{\sqrt{T/u}}{m}, & q < q_{\text{thr}}, \\ 0, & q > q_{\text{thr}}. \end{cases} \quad (\text{A16})$$

Here the value of the threshold momentum $q_{\text{thr}} = \frac{T^{1/3}}{um^{2/3}l^{4/3}}$ is determined by the condition that the energy level broadening (A16) exceeds the nonlinear correction $ul^2 q^3$ to the bosonic dispersion relation at momentum q . This reproduces the result found in Ref.^{21,51,52}.

3. Computation of the thermal conductivity

Now we turn to computation of the thermal conductivity. We decompose the source $S(x)$ term in Eq.(A11) into a part parallel

$$S_{\parallel} = \frac{\pi|x|}{\sinh(\pi x)} \frac{u \nabla T}{T},$$

and perpendicular to the momentum zero mode

$$S_{\perp} = \frac{16\pi^3 l^2 T \nabla T}{5u} \frac{|x|(1-5x^2)}{\sinh(\pi x)}. \quad (\text{A17})$$

Similarly we decompose the sought after solution f into f_{\parallel} and f_{\perp} . Within the relaxation-time approximation the solution of the bosonic kinetic equation is given by

$$f_{\parallel} = -\frac{S_{\parallel}}{i\omega} \quad \text{and} \quad f_{\perp} = \frac{S_{\perp}}{\tau_B^{-1}(q) - i\omega}. \quad (\text{A18})$$

We have checked that this approximate result is in excellent agreement with the exact solution obtained by inverting the full collision integral operator numerically.

The ‘‘longitudinal’’ part of the correction to the distribution function, f_{\parallel} , gives rise to the ballistic contribution to

the thermal conductance, Eq.(7) of the main text. Plugging f_{\perp} from Eq.(A18) into the formula for thermal current, we find the real part of thermal conductivity carried by the bosonic excitations

$$\text{Re } \sigma^B(\omega) \simeq \frac{T^4 l^4}{u^2} \text{Re} \left[\int_0^{T/u} \frac{(dq)}{\tau_B^{-1}(q) - i\omega} \right]. \quad (\text{A19})$$

The momentum integration in Eq.(A19) is cut by the value of the thermal momentum T/u , because beyond it the integrand is exponentially suppressed. By comparing the self-consistent one-into-two boson decay rate with one-into-three boson decay rate one observes that the first one is faster, for $q < q_{\text{thr}}$. Therefore, the integration over momentum in Eq.(A19) is divided into the region $q \geq q_{\text{thr}}$. For $T < T_{\text{FB}}$ it implies that $q_{\text{thr}} > T/u$ and the thermal conductivity alway dominated by one into two bosons decay processes, resulting in

$$\text{Re } \sigma^B(\omega) \simeq \frac{T^{\frac{11}{3}} l^4 u^{-\frac{5}{3}} m_*^{\frac{2}{3}}}{\omega^{\frac{1}{3}}}, \quad \omega < \frac{T^2}{m_* u^2}. \quad (\text{A20})$$

For $T_{\text{FB}} < T < T_H$ where $T_H = u^{\frac{3}{4}} l^{-\frac{5}{4}} m_*^{-\frac{1}{4}}$ the thermal conductivity Eq.(A19) is given by a sum of parts coming from below and above q_{thr} . $\text{Re}(\sigma^B) = I_1(\omega) + I_2(\omega)$. The contribution coming from momenta below q_{thr} is given by

$$I_1(\omega) = \frac{T^{\frac{11}{3}} l^4 u^{-\frac{5}{3}} m_*^{\frac{2}{3}}}{\omega^{\frac{1}{3}}}. \quad (\text{A21})$$

The contribution coming from momenta above q_{thr} is given by

$$I_2(\omega) = \begin{cases} \frac{\gamma l^4 T^{10}}{m_*^4 u^{11}} \frac{1}{\omega^2}, & \omega > \frac{\gamma T^5}{m_*^4 u^8}, \\ \frac{T^{\frac{5}{2}} m_*^2 u l^4}{\omega^{\frac{1}{2}} \gamma^{\frac{1}{2}}}, & \frac{\gamma T^{\frac{11}{3}}}{u^8 m_*^{\frac{16}{3}} l^{\frac{8}{3}}} < \omega < \frac{\gamma T^5}{m_*^4 u^8}, \\ T^{\frac{2}{3}} m_*^{\frac{14}{3}} l^{\frac{16}{3}} u^5 \gamma^{-1}, & \omega < \frac{\gamma T^{\frac{11}{3}}}{u^8 m_*^{\frac{16}{3}} l^{\frac{8}{3}}}. \end{cases} \quad (\text{A22})$$

Thus, the bosonic contribution to the thermal conductivity is given by

$$\text{Re } \sigma^B(\omega) = \begin{cases} \frac{T^{\frac{11}{3}} l^4 u^{-\frac{5}{3}} m_*^{\frac{2}{3}}}{\omega^{\frac{1}{3}}}, & \omega < \frac{\gamma^3 T^9}{m_*^{12} u^{20} l^4}, \\ T^{\frac{2}{3}} m_*^{\frac{14}{3}} l^{\frac{16}{3}} u^5 \gamma^{-1}, & \frac{\gamma^3 T^9}{m_*^{12} u^{20} l^4} < \omega < \frac{\gamma T^{\frac{11}{3}}}{u^8 m_*^{\frac{16}{3}} l^{\frac{8}{3}}}, \\ \frac{T^{\frac{5}{2}} m_*^2 u l^4}{\omega^{\frac{1}{2}} \gamma^{\frac{1}{2}}}, & \frac{\gamma T^{\frac{11}{3}}}{u^8 m_*^{\frac{16}{3}} l^{\frac{8}{3}}} < \omega < \frac{\gamma T^5}{m_*^4 u^8}, \\ \frac{\gamma l^4 T^{10}}{m_*^4 u^{11}} \frac{1}{\omega^2}, & \omega > \frac{\gamma T^5}{m_*^4 u^8}. \end{cases} \quad (\text{A23})$$

For $T \gg T_H$, the thermal conductivity Eq.(A19) is given by a sum of three parts : $q < q_{\text{thr}}$, $q_{\text{thr}} < q < \frac{l^2 T^3}{u^3}$ and $q > \frac{l^2 T^3}{u^3}$. Thus, $\text{Re } \sigma^B(\omega) = I_1(\omega) + I_2(\omega) + I_3(\omega)$. Adding these three contributions, we thus have

$$\text{Re } \sigma^B(\omega) = \begin{cases} \frac{T^{\frac{11}{3}} l^4 u^{-\frac{5}{3}} m_*^{\frac{2}{3}}}{\omega^{\frac{3}{3}}}, & \omega < \frac{\gamma^3 T^{\frac{17}{3}} l^{-\frac{20}{3}} u^{-16}}{m_*^{\frac{34}{3}}}, \\ T^{\frac{16}{9}} m_*^{\frac{40}{9}} l^{\frac{56}{9}} u^{\frac{11}{3}} \gamma^{-1}, & \frac{\gamma^3 T^{\frac{17}{3}} l^{-\frac{20}{3}} u^{-16}}{m_*^{\frac{34}{3}}} < \omega < \frac{\gamma T^{\frac{23}{9}}}{u^{\frac{20}{3}} m_*^{\frac{46}{9}} l^{\frac{32}{9}}}, \\ \frac{T^{\frac{14}{5}} l^{\frac{24}{5}} m_*^{\frac{12}{5}} u}{\omega^{2/5} \gamma^{3/5}}, & \frac{\gamma T^{\frac{23}{9}}}{u^{\frac{20}{3}} m_*^{\frac{46}{9}} l^{\frac{32}{9}}} < \omega < \frac{\gamma l^7 T^{12}}{m_*^4 u^{15}}, \\ \frac{l^2 u^7 m_*^4}{T^2 \gamma}, & \frac{\gamma l^7 T^{12}}{m_*^4 u^{15}} < \omega < \frac{\gamma l^4 T^9}{m_*^4 u^{12}}, \\ \frac{T^{\frac{5}{2}} m_*^2 u l^4}{\omega^{\frac{1}{2}} \gamma^{\frac{1}{2}}}, & \frac{\gamma l^4 T^9}{m_*^4 u^{12}} < \omega < \frac{\gamma T^5}{m_*^4 u^8}, \\ \frac{\gamma l^4 T^{10}}{m_*^4 u^{11}} \frac{1}{\omega^2}, & \frac{\gamma T^5}{m_*^4 u^8} < \omega. \end{cases} \quad (\text{A24})$$

Appendix B: Kinetic theory for fermionic excitations

1. Refermionization

The bosonized Hamiltonian (A3) can be recast in terms of fermionic operators as

$$R_q = \sum_k c_{R,k}^\dagger c_{R,k+q}, \quad L_q = \sum_k c_{L,k}^\dagger c_{L,k+q}. \quad (\text{B1})$$

This results in a refermionised Hamiltonian

$$\begin{aligned} H &= \sum_k \epsilon_{R,k} : c_{R,k}^\dagger c_{R,k} :_F + \frac{1}{L} \sum_{\mathbf{k}} \Gamma_{\mathbf{k}}^{F,RR} : c_{R,k_1}^\dagger c_{R,k_2}^\dagger c_{R,k_2'} c_{R,k_1'} :_F \\ &+ \frac{1}{L} \sum_{\mathbf{k}} \Gamma_{\mathbf{k}}^{F,RL} : c_{R,k_1}^\dagger c_{L,k_2}^\dagger c_{L,k_2'} c_{R,k_1'} :_F + \frac{1}{L^2} \sum_{\mathbf{k}} \Gamma_{\mathbf{k}}^{F,RRR} : c_{R,k_1}^\dagger c_{R,k_2}^\dagger c_{R,k_3}^\dagger c_{R,k_3'} c_{R,k_2'} c_{R,k_1'} :_F \\ &+ \frac{1}{L^2} \sum_{\mathbf{k}} \Gamma_{\mathbf{k}}^{F,RRL} : c_{R,k_1}^\dagger c_{R,k_2}^\dagger c_{L,k_3}^\dagger c_{L,k_3'} c_{R,k_2'} c_{R,k_1'} :_F + (R \longleftrightarrow L). \end{aligned} \quad (\text{B2})$$

We denote by \mathbf{k} in each of vertices $\Gamma_{\mathbf{k}}^{F,\dots}$ the full set of all momenta of the fermionic operators involved. As shown in Ref.³⁴ the dominant vertex for energy relaxation is $\Gamma_{\mathbf{k}}^{F,RRL}$. In the bosonic description it corresponds to 1 boson going into 3 bosons scattering process, e.g. Eq.(A4).

$$\Gamma_{\mathbf{k}}^{F,RRL} = \frac{5\alpha l^2 \pi^2 (k_1 - k_2)(k_1' - k_2')}{16m_*^2 u (k_3 - k_3')} \times [(k_1 - k_2)^2 - (k_1' - k_2')^2]. \quad (\text{B3})$$

2. Kinetic equation for composite fermions

Using the Keldysh formalism, one can derive a kinetic equation for the fermionic distribution $N_k(x, t)$

$$N(k, x, t) = \int_{-\infty}^{\infty} \frac{d(k_1 - k_2)}{2\pi} e^{i(k_1 - k_2)x} \langle c_{k_1}^\dagger(t) c_{k_2}(t) \rangle, \quad (\text{B4})$$

where $k = \frac{k_1 + k_2}{2}$ and the operators c_k and c_k^\dagger are defined in Eq.(B2). By repeating the standard steps of Keldysh formalism with the Hamiltonian (B2) one derives the kinetic equation for composite fermions

$$\frac{\partial N_k}{\partial t} + v_k \frac{\partial N_k}{\partial x} = I[N_k]. \quad (\text{B5})$$

Here $v_k = \partial_k \epsilon_k$ is a velocity of fermions, $\epsilon_k = \frac{k^2}{2m_*} - \frac{k_F^2}{2m_*}$, and $k_F = m_* u$. The fermionic collision integral $I[N]$ is given by

$$I[N] = I_{\text{out}}[N] + I_{\text{in}}[N]. \quad (\text{B6})$$

Here

$$I_{\text{out}}[N]_k = - \sum_{k_2, k_3, k', k'_2, k'_3} W_{kk_2k_3}^{k'k'_2k'_3} N_k N_{k_2} N_{k_3} (1 - N_{k'}) (1 - N_{k'_2}) (1 - N_{k'_3})$$

is outgoing

$$I_{\text{in}}[N]_k = \sum_{k_2, k_3, k', k'_2, k'_3} W_{kk_2k_3}^{k'k'_2k'_3} (1 - N_k) (1 - N_{k_2}) (1 - N_{k_3}) N_{k'} N_{k'_2} N_{k'_3}$$

and incoming parts. The matrix element of three fermion collision³⁴ is given by

$$W_{kk_2k_3}^{k'k'_2k'_3} = \frac{\gamma l^4}{m_*^2 u} (k_2 - k)^2 (k'_2 - k')^2 \delta(k_2 + k - k'_2 - k') \delta(k_3 - k'_3).$$

Near the equilibrium one can linearize the collision integral using the ansatz

$$N = n + gf. \quad (\text{B7})$$

Here n denotes the local equilibrium Fermi-Dirac distribution $n_k = \frac{1}{e^{\epsilon_k/T} + 1}$ and $g_k = \sqrt{n_k(1 - n_k)} = \frac{1}{2 \cosh \epsilon_k/2T}$. After Fourier transforming it in time, the linearized Boltzmann equation reads

$$-i\omega f_k + B_k^F \frac{\nabla T}{T^2} = \mathcal{I}[f]_k, \quad (\text{B8})$$

where

$$B_k^F = v_k \epsilon_k g_k. \quad (\text{B9})$$

and the linearized collision integral \mathcal{I} is

$$\begin{aligned} \mathcal{I}[f]_k &= \frac{\gamma T l^4}{m_*^2 u^2} \int_{-\infty}^{\infty} dk_2 \int_{-\infty}^{\infty} dk' \int_{-\infty}^{\infty} dk'_2 (k - k_2)^2 (k' - k'_2)^2 \delta(k + k_2 - k' - k'_2) \\ &\quad g(k_2) g(k') g(k'_2) \left(\frac{f(k)}{g(k)} + \frac{f(k_2)}{g(k_2)} - \frac{f(k')}{g(k')} - \frac{f(k'_2)}{g(k'_2)} \right). \end{aligned} \quad (\text{B10})$$

On the level of diagonal approximation, we find the decay rate

$$\tau_F^{-1}(k) = \frac{\gamma T l^4}{g(k) m_*^2 u^2} \int_{-\infty}^{\infty} dk_2 \int_{-\infty}^{\infty} dk' \int_{-\infty}^{\infty} dk'_2 (k - k_2)^2 (k' - k'_2)^2 \delta(k + k_2 - k' - k'_2) g(k_2) g(k') g(k'_2). \quad (\text{B11})$$

This yields fermionic life time

$$\frac{1}{\tau_F(q)} = \begin{cases} \frac{\gamma l^4 T k^6}{m_*^2 u^2}, & k > \frac{T}{u}, \\ \frac{\gamma l^4 T^7}{m_*^2 u^8}, & k < \frac{T}{u}. \end{cases} \quad (\text{B12})$$

reproducing the results of Ref.^{26,27,34,53}. We have also numerically studied the life time employing full kernel and found that the results (B12) hold.

Next, we compute the thermal conductivity in the fermionic channel. Since fermions are massive particles, one should impose a zero momentum transfer condition⁵⁸. It is achieved by subjecting the system to the gradient of chemical potential $\nabla \mu$. After this procedure, we are left with \mathcal{B}^F that is a part of B^F orthogonal to the *momentum* zero mode $\phi_p = \frac{1}{\sqrt{2m_* T k_F}} k g_k$.

In the orthogonal subspace, we now further decompose it into parts parallel and perpendicular to the *number* zero mode $\phi_n = \sqrt{\frac{k_F}{2m_* T}} \text{sgn}(k) g_k$. This results in the decomposition $\mathcal{B}^F = \mathcal{B}_{\parallel}^F + \mathcal{B}_{\perp}^F$. To leading order in T ,

$$\mathcal{B}_{\parallel}^F = \frac{\sqrt{2k_F^{\frac{5}{2}} T^{\frac{1}{2}}}}{m_*^{\frac{3}{2}}} (\phi_p - \phi_n), \quad \mathcal{B}_{\perp}^F = B^F - \frac{\sqrt{2m_* \pi^2 T^{\frac{5}{2}}}}{3k_F^{\frac{3}{2}}} \phi_p - \mathcal{B}_{\parallel}^F. \quad (\text{B13})$$

We now substitute this decomposition into Eq.(B8) and compute the thermal conductivity.

3. Computation of the thermal conductivity

Within the diagonal approximation one can solve the Boltzmann equation Eq.(B8)

$$f_{\text{bal}} = \frac{\mathcal{B}_{\parallel}^{\mathcal{F}}}{-i\omega} \frac{\nabla T}{T^2}, \quad f_{\perp} = \frac{\nabla T}{T^2} \frac{\mathcal{B}_{\perp}^{\mathcal{F}}}{\tau_F^{-1} - i\omega}. \quad (\text{B14})$$

Thus, the ballistic part of the thermal current is given by

$$J_{\text{bal}} = \frac{\pi}{3} \frac{T u}{i\omega} \nabla T.$$

The ballistic part of the thermal current matches the one found within the bosonic approach. This happens because in both descriptions it is fully controlled by a corresponding (bosonic and fermionic) momentum zero modes.

The real part of thermal conductivity is thus given by

$$\text{Re } \sigma^F(\omega) \simeq \frac{T^2}{m_*^2 u^2} \text{Re} \int_0^{\frac{T}{u}} \frac{(dq)}{\tau_F(q)^{-1} - i\omega}. \quad (\text{B15})$$

Employing Eq.(B12) for the fermionic life time, one finds

$$\text{Re } \sigma^F(\omega) = \begin{cases} \frac{1}{\omega^2} \frac{\gamma T^{10} l^4}{u^{11} m_*^4}, & \omega > \frac{\gamma l^4 T^7}{m_*^2 u^8} \quad (\text{regime F1}) \\ \frac{u^5}{\gamma T^4 l^4}, & \omega < \frac{\gamma l^4 T^7}{m_*^2 u^8} \quad (\text{regime F2}). \end{cases} \quad (\text{B16})$$

Appendix C: Final thermal conductivity: bosons vs fermions

As we showed above, there are two channels of the energy transport in 1D electronic fluid: fermionic and bosonic. The resulting contribution to thermal conductivity is given by a sum of bosonic and fermionic parts. For the imaginary part of the thermal conductivity, both fermionic and bosonic channels yield identical results, and therefore one may use either description. For the real part of the thermal conductivity, this is not the case. However, since $\text{Re } \sigma \sim \tau$, it is automatically determined by the long-living species. Therefore, up to a numerical prefactor, the result can be obtained by summing both contributions. Now we analyze the results for different temperature limits.

1. High temperature regime, $T > T_{\text{FB}}$

For $T_{\text{FB}} < T$, the bosonic description is suitable, $\tau_B(q) > \tau_F(q)$, for all accessible momenta, $q < T/u$. Therefore the real part of thermal conductivity is determined by $\sigma_B(\omega)$.

For $T_{\text{BF}} < T < T_H$, $\sigma_B(\omega)$ is given by Eq.(A23), thus leading to the total thermal conductivity

$$\text{Re } \sigma'(\omega) = \begin{cases} \frac{T^{\frac{11}{3}} l^4 u^{-\frac{5}{3}} m_*^{\frac{2}{3}}}{\omega^{\frac{1}{3}}}, & \omega < \frac{\gamma^3 T^9}{m_*^2 u^{20} l^4}, \\ T^{\frac{2}{3}} m_*^{\frac{14}{3}} l^{\frac{16}{3}} u^5 \gamma^{-1}, & \frac{\gamma^3 T^9}{m_*^2 u^{20} l^4} < \omega < \frac{\gamma T^{\frac{11}{3}}}{u^8 m_*^{\frac{16}{3}} l^{\frac{8}{3}}}, \\ \frac{T^{5/2} m_*^2 u l^4}{\omega^{\frac{1}{2}} \gamma^{\frac{1}{2}}}, & \frac{\gamma T^{\frac{11}{3}}}{u^8 m_*^{\frac{16}{3}} l^{\frac{8}{3}}} < \omega < \frac{\gamma T^5}{m_*^4 u^8}, \\ \frac{\gamma T^{10} l^4}{\omega^2 u^{11} m_*^4}, & \omega > \frac{\gamma T^5}{m_*^4 u^8}. \end{cases} \quad (\text{C1})$$

These results lead to the total thermal conductivity shown in Fig.3.

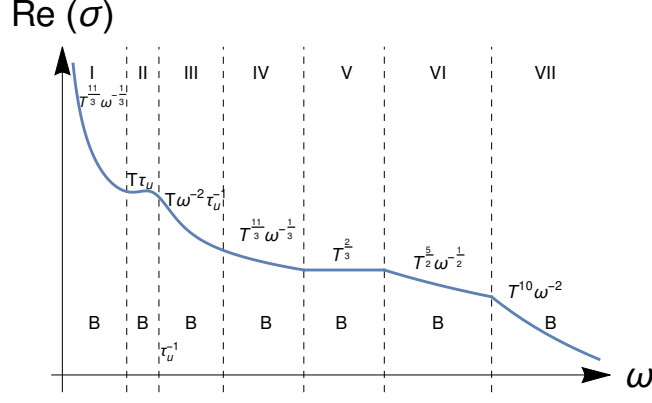


FIG. 3: Real part of $\sigma(\omega)$ at $T_{FB} < T < T_H$, we omit the constants for clarity. Label B indicates that dominant contribution is bosonic. In Regions II, III the contribution of the momentum zero mode to σ is significant, while other regions are dominated by finite energy bosonic modes, e.g. Eq.(C1).

For $T \gg T_H$ the bosonic conductivity $\sigma_B(\omega)$ is given by Eq.(A24), thus

$$\text{Re } \sigma'(\omega) = \begin{cases} \frac{T^{\frac{11}{3}} l^4 u^{-\frac{5}{3}} m_*^{\frac{2}{3}}}{\omega^{\frac{1}{3}}}, & \omega < \frac{\gamma^3 T^{\frac{17}{3}} l^{-\frac{20}{3}} u^{-16}}{m_*^{\frac{34}{3}}}, \\ T^{\frac{16}{9}} m_*^{\frac{40}{9}} l^{\frac{56}{9}} u^{\frac{11}{3}} \gamma^{-1}, & \frac{\gamma^3 T^{\frac{17}{3}} l^{-\frac{20}{3}} u^{-16}}{m_*^{\frac{34}{3}}} < \omega < \frac{\gamma T^{\frac{23}{9}}}{u^{\frac{20}{3}} m_*^{\frac{46}{9}} l^{\frac{32}{9}}}, \\ \frac{T^{\frac{14}{5}} l^{\frac{24}{5}} m_*^{\frac{12}{5}} u}{\omega^{2/5} \gamma^{3/5}}, & \frac{\gamma T^{\frac{23}{9}}}{u^{\frac{20}{3}} m_*^{\frac{46}{9}} l^{\frac{32}{9}}} < \omega < \frac{\gamma l^7 T^{12}}{m_*^4 u^{15}}, \\ \frac{l^2 u^7 m_*^4}{T^2 \gamma}, & \frac{\gamma l^7 T^{12}}{m_*^4 u^{15}} < \omega < \frac{\gamma l^4 T^9}{m_*^4 u^{12}}, \\ \frac{T^{\frac{5}{2}} m_*^2 u l^4}{\omega^{\frac{1}{2}} \gamma^{\frac{1}{2}}}, & \frac{\gamma l^4 T^9}{m_*^4 u^{12}} < \omega < \frac{\gamma T^5}{m_*^4 u^8}, \\ \frac{\gamma l^4 T^{10}}{m_*^4 u^{11}} \frac{1}{\omega^2}, & \frac{\gamma T^5}{m_*^4 u^8} < \omega. \end{cases} \quad (\text{C2})$$

The resulting thermal conductivity is schematically shown in Fig. 4.

2. Low temperature regime, $T < T_{FB}$

The story is different for $T < T_{FB}$. In the high frequency limit, fermions dominate the thermal conductivity. Below a critical frequency, $\omega_* = \gamma^3 T^{23} m_*^2 l^{24} u^{-20}$ bosons dominate it. At the crossover frequency $\tau_B(\omega_*) > \tau_F(\omega_*)$, which implies that the bosons are the good quasi-particles and the dominant contribution was found correctly. The inequality remains true even at lower frequencies as the bosonic excitations become more long-lived at low frequencies while the fermionic lifetime remains constant. The result is

$$\text{Re } \sigma'(\omega) = \begin{cases} \frac{T^{\frac{11}{3}} l^4 u^{-\frac{5}{3}} m_*^{\frac{2}{3}}}{\omega^{\frac{1}{3}}}, & \omega < \frac{\gamma^3 T^{23} m_*^2 l^{24}}{u^{20}}, \\ \frac{u^5}{\gamma T^4 l^4}, & \frac{\gamma^3 T^{23} m_*^2 l^{24}}{u^{20}} < \omega < \frac{\gamma l^4 T^7}{m_*^2 u^8}, \\ \frac{1}{\omega^2} \frac{\gamma T^{10} l^4}{u^{11} m_*^4}, & \omega > \frac{\gamma l^4 T^7}{m_*^2 u^8}. \end{cases} \quad (\text{C3})$$

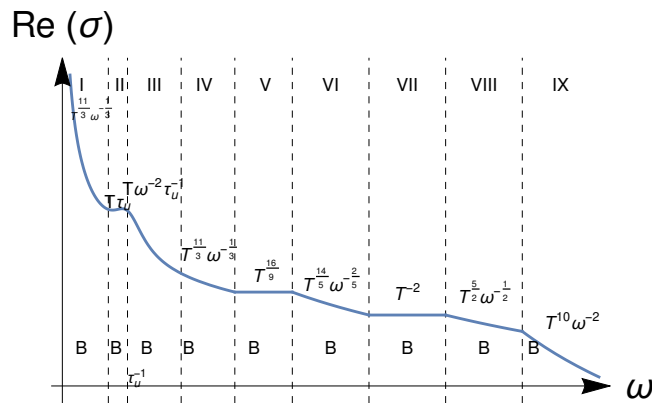


FIG. 4: Real part of $\sigma(\omega)$ at $T \gg T_H$, we omit the constants for clarity. Label B indicates that dominant contribution is bosonic. In Regions II, III the contribution of the momentum zero mode to σ is significant, while other regions are dominated by finite energy bosonic modes, e.g. Eq.(C2).

It is worth mentioning that for high frequencies, the real part of thermal conductivity computed solely with bosonic sector matches the one calculated within the fermionic one.

-
- ¹ K. Schwab, E. Henriksen, J. Worlock, and M. Roukes, *Measurement of the quantum of thermal conductance*, Nature **404**, 974 (2000).
 - ² M. Meschke, W. Guichard, J. P. Pekola, *Singlemode heat conduction by photons*. Nature **444**, 187-190 (2006).
 - ³ Jezouin, S. et al. *Quantum Limit of Heat Flow Across a Single Electronic Channel*, Science **342**, 601 (2013).
 - ⁴ Cui, L. et al. *Quantized thermal transport in single-atom junctions*, Science **355**, 1192 (2017).
 - ⁵ E. Sivre, A. Anthore, F.D. Parmentier, A. Cavanna, U. Gennser, A. Ouerghi, Y. Jin, and F. Pierre, *Heat Coulomb Blockade of One Ballistic Channel*, Nature **14**, 145 (2018).
 - ⁶ C. Altimiras, H. le Sueur, U. Gennser, A. Anthore, A. Cavanna, D. Mailly, and F. Pierre, *Energy Relaxation in the Integer Quantum Hall Regime*, Phys. Rev. Lett. **109**, 026803 (2012).
 - ⁷ V. Venkatachalam, S. Hart, L. Pfeiffer, K. West, and A. Yacoby, *Local thermometry of neutral modes on the quantum Hall edge*, Nature Phys. **8**, 676 (2012).
 - ⁸ H. Inoue, A. Grivnin, Y. Ronen, M. Heiblum, V. Umansky, and D. Mahalu, *Proliferation of neutral modes in fractional quantum Hall states*, Nature Comm. **5**, 4067 (2014).
 - ⁹ M. Banerjee, M. Heiblum, A. Rosenblatt, Y. Oreg, D. Feldman, A. Stern and V. Umansky, *Observed Quantization of Anyonic Heat Flow*, Nature, **545**, 75 (2017).
 - ¹⁰ A. Rosenblatt, F. Lafont, I. Levkivskiy, R. Sabo, I. Gorman, D. Baniitt, M. Heiblum, V. Umansky, *Transmission of heat modes across a potential barrier*, Nature, **8**, 2251 (2017).
 - ¹¹ M. Banerjee, M. Heiblum, V. Umansky, D. Feldman, Y. Oreg, and A. Stern, *Observation of half-integer thermal Hall conductance*, Nature, **559**, 205 (2018).
 - ¹² Y.K. Koh, and D. G. Cahill, *Frequency dependence of the thermal conductivity of semiconductor alloys*, Phys. Rev. B, **76**, 75207 (2007).
 - ¹³ A. J. Minnich, J. A. Johnson, A. J. Schmidt, K. Esfarjani, M. S. Dresselhaus K. A. Nelson and G. Chen, *Thermal Conductivity Spectroscopy Technique to Measure Phonon Mean Free Paths*, Phys. Rev. Lett., **107**, 95901 (2011).
 - ¹⁴ K. T. Regner, D. P. Sellan, Z. Su, C. H. Amon, A. J. H. McGaughey, J. A. Malen, *Broadband phonon mean free path contributions to thermal conductivity measured using frequency domain thermoreflectance*, Nature Communications, **4**, 1640 (2013).
 - ¹⁵ E. Fermi, J. Pasta, S. Ulam, and M. Tsingou, *Studies of non-linear problems*, FPU, Document LA-1940. Los Alamos National Laboratory, (1955).
 - ¹⁶ O. Narayan and S. Ramaswamy, *Anomalous heat conduction in one-dimensional momentum-conserving systems*, Phys. Rev. Lett. **89**, 200601 (2002).
 - ¹⁷ Herbert Spohn, *Nonlinear Fluctuating Hydrodynamics for Anharmonic Chains*, Journal of Statistical Physics, **154** (2014).
 - ¹⁸ T. Mai, A. Dhar, O. Narayan, *Equilibration and Universal Heat Conduction in Fermi-Pasta-Ulam Chains*, Phys. Rev. Lett., **98**, 184301 (2007).
 - ¹⁹ H. van Beijeren, Phys. Rev. Lett. **108**, 180601 (2012).
 - ²⁰ M. Kulkarni and A. Lamacraft, *From GPE to KPZ: finite temperature dynamical structure factor of the 1D Bose gas*, Phys. Rev. A **88**, 021603 (2013).
 - ²¹ M. Arzamasovs, F. Bovo, D.M. Gangardt, *Kinetics of Mobile Impurities and Correlation Functions in One-Dimensional Superfluids at Finite Temperature*, Phys. Rev. Lett. **112**, 170602 (2014).
 - ²² T. Giamarchi, *Quantum Physics in One Dimension*, (Clarendon Press Oxford, 2004).

- ²³ I.V. Protopopov, D. B. Gutman, M. Oldenburg, and A.D. Mirlin, *Dissipationless kinetics of one-dimensional interacting fermions*, Phys. Rev. B **89**, 161104 (2014).
- ²⁴ I.V. Protopopov, D.B. Gutman, P. Schmitteckert, and A.D. Mirlin, *Dynamics of waves in 1D electron systems: Density oscillations driven by population inversion*, Phys. Rev. B **87**, 045112 (2013).
- ²⁵ A. Imambekov and L.I. Glazman, *Universal Theory of Nonlinear Luttinger Liquids*, Science **323**, 228 (2009); *Phenomenology of One-Dimensional Quantum Liquids Beyond the Low-Energy Limit*, Phys. Rev. Lett. **102**, 126405 (2009).
- ²⁶ A. Imambekov, T.L. Schmidt, and L.I. Glazman, *One-dimensional quantum liquids: Beyond the Luttinger liquid paradigm*, Rev. Mod. Phys **84**, 1253 (2012)
- ²⁷ M. Khodas, M. Pustilnik, A. Kamenev, L.I. Glazman, *Fermi-Luttinger liquid: Spectral function of interacting one-dimensional fermions*, Phys. Rev. B **76**, 155402 (2007).
- ²⁸ M. Filippone, F. Hekking, and A. Minguzzi, *Violation of the Wiedemann-Franz law for one-dimensional ultracold atomic gases*, Phys. Rev. A **93**, 011602 (2016).
- ²⁹ L.D. Landau, J. Phys. USSR **5**, 71 (1941); Sov. Phys. ZhETF **11**, 592 (1941).
- ³⁰ E.M. Lifshitz and L.P. Pitaevskii, *Statistical Physics, Part 2*, (Elsevier, Oxford, 1980).
- ³¹ M. Schick, Phys. Rev. **166**, 404 (1968).
- ³² B. Sakita, *Quantum Theory of Many-variable Systems and Fields* (World Scientific, Singapore, 1985).
- ³³ A. Jevicki and B. Sakita, Nuc. Phys. B **165**, 511 (1980).
- ³⁴ I. V. Protopopov, D. B. Gutman and A. D.Mirlin, *Relaxation in Luttinger liquids: Bose-Fermi duality*. Phys. Rev. B. **90**, 125113 (2014).
- ³⁵ A.V. Rozhkov, Phys. Rev. B **77**, 125109 (2008); Phys. Rev. B **74**, 245123 (2006); Eur.Phys.J. **47** , 193 (2005).
- ³⁶ The fermionic quasiparticles introduced in this way are advantageous over the original electrons of the model because their interaction vanishes in the low-energy limit. In particular, they have flat density of states at the Fermi surface.
- ³⁷ F.D.M Haldane, *Luttinger liquid theory of one-dimensional quantum fluids*, Journal of Physics C : Solid State Physics, **14**, 2585 (1981).
- ³⁸ M. Stone, *Bosonization* (World Scientific, 1994).
- ³⁹ J. von Delft and H. Schoeller, *Bosonization for beginners-refermionization for experts*, Annalen Phys. **7**, 225 (1998).
- ⁴⁰ A. O. Gogolin, A. A. Nersesyan, and A. M. Tsvelik, *Bosonization in Strongly Correlated Systems*, (University Press, Cambridge 1998).
- ⁴¹ K. A. Matveev and A. V. Andreev, *Equilibration of a spinless Luttinger liquid*, Phys. Rev. B **85**, 041102 (2012)
- ⁴² T. Micklitz, J. Rech, and K.A. Matveev, *Transport properties of partially equilibrated quantum wires*, Phys. Rev B **81**, 115313 (2010).
- ⁴³ K.A. Matveev and A.V. Andreev, *Scattering of hole excitations in a one-dimensional spinless quantum liquid*, Phys. Rev B **86**, 045136 (2012).
- ⁴⁴ K.A. Matveev, A.V. Andreev and A.D. Klironomos, *Scattering of charge and spin excitations and equilibration of a one-dimensional Wigner crystal*, Phys. Rev. B **90**, 035148 (2014).
- ⁴⁵ K.A. Matveev and A.V. Andreev, *Hybrid Sound Modes in One-Dimensional Quantum Liquids*, Phys. Rev. Lett. **121**, 026803 (2018).
- ⁴⁶ C.L. Kane and M.P.A. Fisher, *Thermal Transport in a Luttinger Liquid*, Phys. Rev. Lett. **76**, 3192 (1996).
- ⁴⁷ A. Levchenko, T. Micklitz, J. Rech and K.A. Matveev, *Transport in partially equilibrated inhomogeneous quantum wires*, Phys. Rev. B **82**, 115413 (2010).
- ⁴⁸ A. Pereverzev, *Fermi-Pasta-Ulam β lattice: Peierls equation and anomalous heat conductivity*, Phys. Rev. E, **68**, 056124 (2003).
- ⁴⁹ Herbert Spohn and Jani Lukkarinen, *Anomalous energy transport in the FPU- β chain*, Communications on Pure and Applied Mathematics, **61**, 1753 (2008).
- ⁵⁰ J. Lin, K. A. Matveev, M. Pustilnik, *Thermalization of Acoustic Excitations in a Strongly Interacting One-Dimensional Quantum Liquid*, Phys. Rev. Lett. **110**, 016401 (2013).
- ⁵¹ A. F. Andreev, *The hydrodynamics of two and one dimensional liquids*, Sov. Phys. JETP **51**, 1038 (1980).
- ⁵² K. Samokhin, *Lifetime of excitations in a clean Luttinger liquid*, J. Phys. Condens. Matter **10**, 533 (1998).
- ⁵³ A.M. Lunde, K. Flensberg, and L.I. Glazman, Phys. Rev. B **75**, 245418 (2007).
- ⁵⁴ S. Rickmoy, I.V. Protopopov, D.B. Gutman and A.D. Mirlin, *Pulse propagation in electronic fluid*, to be published.
- ⁵⁵ K. A. Matveev and Z. Ristivojevic, *Thermal conductivity of the degenerate one-dimensional Fermi gas*, arXiv:1901.08136.
- ⁵⁶ A. Kamenev, *Field Theory of Non Equilibrium Systems*, Cambridge University Press (2011)
- ⁵⁷ J. Rammer and H. Smith, *Quantum field-theoretical methods in transport theory of metals*, Rev. Mod. Phys. **58**, 323 (1986).
- ⁵⁸ L.D. Landau and E.M. Lifshitz, *Statistical Physics*, (Elsevier,Oxford,1990).